JOURNAL OF MATERIALS SCIENCE 28 (1993) 1421–1429

Review
Tensile dilatometric studies of deformation in polymeric materials and their composites

S. I. NAQUI, I. M. ROBINSON
ICI Wilton Research Centre, P.O. Box 90, Wilton, Cleveland TS6 8JE, UK

The theory for volume changes in deformation for polymeric materials is presented, together with a brief literature review of the general area of tensile dilatometry. The theory has been used to enable the prediction of the volumetric response of a material to a deformation, which allows for the detection of the onset of cavitation (volume increasing)-type mechanisms in materials displaying such responses. A series of experiments has been performed using an instrumented tensile dilatometry technique on PMMA and on talc-filled reinforced polypropylene at 23 and 60 °C. The engineering constants, tensile modulus and lateral contraction ratio were measured and found to be viscoelastic. The determination of strain in three mutually perpendicular directions during the instrumented tensile test resulted in the measurement and prediction of the volumetric strain response with applied load. A significant cavitation-type mechanism was recorded in the case of the talc-filled reinforced polypropylene, whereas PMMA showed a deviatoric type mechanism. The volume strain has been found to be directly related to the bulk modulus for these materials. Finally, a new method of presenting volumetric strain versus applied stress data is shown and its relevance explained.

1. Introduction

For isotropic, homogeneous materials the state of elasticity in the bulk can be described by four independent constants, the tensile modulus, E, the shear modulus, G, the bulk modulus, K, and the lateral contraction ratio, ν. These constants are related by a series of expressions that are well established, so that in principle, if any two constants are known, the other two may be calculated [1, 2]. Consequently, none of these constants are more important than any other, though some are experimentally easier to determine than others. In the case of polymeric materials and their derivatives, these constants are inherently viscoelastic in nature [3, 4] so they are properly described as being pseudoelastic constants.

In the small deformation limit, an applied stress may be analysed into tensorial components of the sum of the mean normal hydrostatic tensor and the deviatoric tensor [1, 2]. The hydrostatic stress results in a dilational (volume increasing) response of the material, while the deviatoric (shear) stress results only in a change of shape, not volume. Any small deformation can be related to these two components of stress. However, in the large deformation limit, the hydrostatic tensile stress causing dilation may result in cavitation-type mechanisms, producing a rapid increase in volume which leads eventually to fracture; the deviatoric stresses may result in shear yielding as the principle failure mechanism. Often in a material under large deformation, one of these principal mechanisms will dominate the failure process. Consequently, the characterization of the dilational response of a material to an applied stress may lead to an appreciation of the deformation mechanisms present in the bulk of the material.

The dilational response of a material to an applied stress can be understood in terms of the volumetric strain, V_s. This concept is explained below from first principles and is then related to the elastic constants of a material. A review is then given of the reported dilatometric studies of polymers in the scientific literature. Finally, an improvement in the experimental method of tensile dilatometry is reported, together with some data for poly(methyl methacrylate) (PMMA) and for a 40% talc-filled polypropylene composite.

2. Theory for volume changes during deformation

The volume strain increase in the bulk of a material resulting from the application of a tensile stress to a specimen can be described as follows [1, 2, 5–8]

$$V_s = (1 + \varepsilon_A)(1 + \varepsilon_W)(1 + \varepsilon_T) - 1 \quad (1)$$

If the material under consideration is assumed to be isotropic, the fundamental elastic constants such as

0022–2461

modulus, E, and lateral contraction ratio, ν, are direction independent. From the assumption of isotropy the lateral contraction ratios in the width and thickness directions are equivalent

$$\nu = -\frac{\varepsilon_W}{\varepsilon_A} = -\frac{\varepsilon_T}{\varepsilon_A} \quad (2)$$

Consequently, Equation 1 can be rewritten as

$$V_s = (1 + \varepsilon_A)(1 - \nu\varepsilon_A)^2 - 1 \quad (3)$$

On expansion of this equation, the volume strain can be expressed as

$$V_s = \varepsilon_A(1 - 2\nu) + \varepsilon_A^2(\nu^2 - 2\nu) + \varepsilon_A^3\nu^2 \quad (4)$$

Thus it can be seen that the volume strain expression contains first, second- and third-order terms that are based on the axial strain and lateral contraction ratio, ν. Conventionally, only the first-order term is retained, although the second-order term can be measured.

The data collected from a tensile test conventionally measures the stress–strain function. If a lateral strain gauge is added to the experiment, the lateral contraction ratio can be determined, together with the volume strain response. By comparing the volume strain function with an applied deformation, it is possible to monitor the mechanisms involved in the bulk deformation of polymers. The major contribution to the increase of volume strain for small deformation is the dilational response due to hydrostatic tension in the bulk of the material under stress, which is governed by the lateral contraction ratio, as defined by Equation 4. Consequently if ν is known, it is possible to predict the dilational response of a material to an applied tensile stress, in the low deformation limit. Monitoring the point of departure between the predicted and measured volume strain response to an applied stress gives an indication of the load required to initiate a change in deformation mechanism in a material. These may include cavitation-type mechanisms such as crazing, voiding, microdebonding, which lead to an increase of volume strain with deformation in excess of that due to dilation. Alternatively deviatoric mechanisms such as shear-band formation [6] will lead to a constant value of volume strain with deformation.

Consequently, the volume strain due to the dilational response can be calculated from the following expression if ν is known by substituting this value into Equation 4

$$V_{S\,DIL} = \varepsilon_A(1 - 2\nu) + \varepsilon_A^2(\nu^2 - 2\nu) + \varepsilon_A^3\nu^2 \quad (5)$$

Thus the component of volume strain due to deviatoric or cavitation-type mechanisms can be calculated from the difference in Equations 1 (the measured volume strain) and 5 (the predicted volume strain)

$$V_{S\,CAV/DEV} = V_S - V_{S\,DIL} \quad (6)$$

If cavitation is the principal deformation mechanism, then Equation 6 will produce a positive contribution to the volume strain predicted from Equation 5 as voiding occurs. If deviatoric mechanisms occur, then Equation 6 will produce a negative contribution to the volume strain predicted from Equation 5 as shear banding occurs. This is shown schematically in Fig. 1.

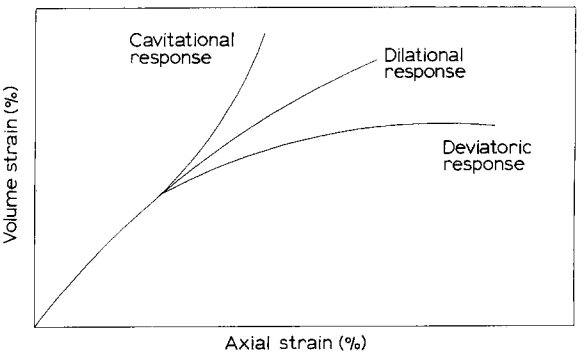

Figure 1 Schematic representation of the volume strain–axial strain deformation of a material undergoing either bulk cavitation or yield.

Alternatively, the term for the axial strain in Equation 4 can be substituted using the relationship between tensile modulus and the true stress

$$\varepsilon_A = \frac{\sigma_T}{E} \quad (7)$$

the volume strain becomes

$$V_S = \left(1 + \frac{\sigma_T}{E}\right)\left(1 - \frac{\nu\sigma_T}{E}\right)^2 - 1 \quad (8)$$

This may also be expanded to

$$V_S = \frac{\sigma_T}{E}(1 - 2\nu) + \left(\frac{\sigma_T}{E}\right)^2(\nu^2 - 2\nu) + \left(\frac{\sigma_T}{E}\right)^3\nu^2 \quad (9)$$

The volume strain expression can also be seen to depend on first-, second- and third-order terms containing the axial stress and the elastic constants, modulus and lateral contraction ratio, ν. Assuming that under small deformations the lateral contraction ratio is constant, the increase of volume strain with deformation is directly related to the increase of applied stress. Consequently, the volume strain–axial stress plot allows a determination of the bulk modulus in the region where dilational effects due to the lateral contraction ratio governs the deformation, as described in Section 5.3.

The mechanisms described above such as cavitation or shear banding can be explained by simple inspection of Equation 8. In the low deformation limit, the modulus will be in direct proportion to the applied stress. However, as the stress approaches the yield point the modulus will begin to fall. Consequently, Equation 8 indicates that the volume strain will increase linearly with stress until the yield point. For materials displaying a deviatoric-type response, the volume strain will reach a limiting value as the stress value approaches σ_Y, because the material will continue to deform by changing shape, not volume. Materials that display cavitation-type mechanisms will show a different volume strain response about the yield point. As the stress approaches σ_Y, the cavitation-type mechanisms will produce voiding and the volume strain will increase rapidly with stress. Thus the two deformation mechanisms can be clearly distinguished, as shown schematically in Fig. 2.

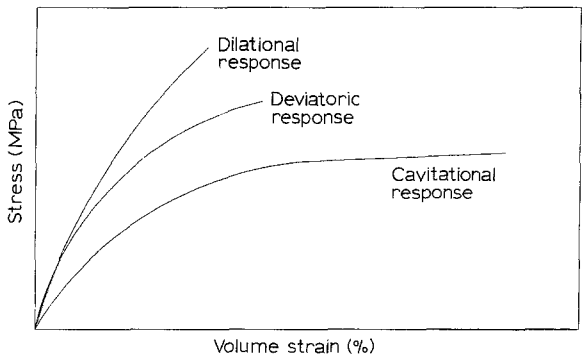

Figure 2 Schematic representation of the volume strain–stress deformation of a material undergoing normal hydrostatic tension and finally yield.

3. Literature review of tensile dilatometric studies of deformation

A number of studies on the deformation mechanisms of unfilled and reinforced polymers have been reported using tensile dilatometry as an investigative technique by a variety of experimental methods. These have included studies by Bucknall and co-workers [8–19], Yee and co-workers [20–23], Heikens and co-workers [24–28], Dekkers and co-workers [29, 30], Moore and co-workers [31–34], Truss and Chadwick [35, 36], Cessna [37], Powers and Caddell [38], Lazzeri et al. [39], Frank and Lehmann [40] and Borggreve *et al.* [41]. A brief report on each author's work is given, followed by some general conclusions.

Bucknall and co-workers [8–19] concentrated their efforts in tensile dilatometry on studying the effect of rubber toughening of plastics (including HIPS, ABS, PP, PMMA and PA66) using a modified creep apparatus to determine the degree of volume strain with deformation. This has often been accompanied by a creep and recovery experiment [9, 10] in an attempt to define the degree of damage caused in the deformation. Cavitation mechanisms, including crazing have been extensively studied, using an Eyring-type approach, with respect to applied stress [8–14]. In addition, void formation in rubber particles has been observed in a rubber-toughened polyamide [18]. The process of shear yielding has also been studied in a range of materials [14–18]. The effects of thermal history on the mechanical properties of PMMA were studied using a volume recovery technique based on creep dilatometry [19].

Yee and co-workers [20–23] have also examined toughening mechanisms in a range of rubber-toughened polymers, including thermoplastics (PC/PE, PXE/HIPS and PA/PPO) and thermosets. The experimental route used has been an instrumented tensile test approach in all studies. Both cavitation and shear yielding have been observed over a range of different strain rates, with the voiding being sensitive to strain rate [20]. In the case of the rubber -toughened epoxy work [21, 23] at low strains the rubber particles were found to produce only shear banding, whereas at high strains the rubber particles cavitated prior to further shear banding.

Heikens and co-workers [24–28] have studied blends of PS/PE and in glass bead particulate composites with PS, PC and SAN copolymer acting as the matrix material. The tensile dilation was measured using a liquid dilatometer described fully in [24]. For the PS/PE blend [25] a combination of crazing and shear band formation was reported. The work based on glass bead particulate composites [26, 28] showed that the particles acted as stress concentrators and the degree of bonding between the two phases controlled the deformation mechanism. Unfilled and well-adhering particle composites showed only shear banding as the principal deformation mechanism. Poorly adhering systems also showed dewetting cavitation in addition to shear banding. In [28] the glass beads were found to be initiation sites for both crazing and shear band yielding, the mechanism again controlled by the degree of adhesion. The kinetics for crazing and shear band deformation were modelled using a simple model and Eyring's theory.

Dekkers and co-workers [29, 30] studied the deformation in toughened PBT/BPA PC blends and in PPO/PA blends. Experimentally, an instrumented tensile test approach was used in all studies. A change from cavitation in the impact modifier particles to shear banding as the principal deformation mechanism was observed as the temperature was increased from $-30\,^{\circ}C$ to $23\,^{\circ}C$.

Hooley *et al.* [31] explored rubber toughening of PMMA, and related their tensile dilatometry results obtained from an instrumented tensile test to fracture mechanics parameters, in order to identify the principal toughening mechanisms. The technique was reviewed in [32] and the instrumented tensile dilatometry test was also applied to failure and fracture mechanisms in discontinuous glass nylon composites [33, 34]. Cavitation mechanisms, due possibly to debonding in the composite, was the principal method of failure measured in these forms of composite.

Truss and Chadwick [35, 36] studied ABS polymers using a instrumented tensile dilatometry approach. The failure mode examined was described to be due to crazing, which was studied at a range of temperatures from -80–$20\,^{\circ}C$ and strain rates.

Cessna [37] studied a range of polymers using tensile tests at a range of strain rates and temperatures (-190–$55\,^{\circ}C$). Both shear yielding and cavitation mechanisms were identified, using an optical experimental approach together with a liquid displacement tensile dilatometer.

Powers and Caddel [38] deformed PE, PC and PMMA and found that a range of lateral contraction ratios were measured for each material, leading to a range of volume changes with applied strain. The PC and PMMA showed volume increasing mechanisms, whereas the high-density PE showed a maximum value for volume increase and then a subsequent decrease.

Frank and Lehmann [40] studied impact-modified PMMA at strain rates of up to 10^5 % min^{-1} in an attempt to examine the various deformation mechanisms. Two principal experimental techniques were used; for low strain rates an instrumented tensile test was used and at the high rates (10^5 % min^{-1}) an optical device attached to a heavy pendulum was used

with the resultant lateral strain was measured using a photodiode system. At strains in excess of 3% it was found that both cavitational and shear deformation processes occurred, with a higher amount of cavitation being found at faster strain rates. These processes were related to the loss of energy stored elastically during deformation.

Borggreve *et al.* [41] used an instrumented tensile test to study nylon-rubber blends in an attempt to measure the degree of cavitation occurring as a function of rubber particle size and strain. The results suggested that a low-modulus and high lateral contraction ratio favoured the creation of voiding in the elastomeric particles.

Lazzeri *et al.* [39] used a modified creep apparatus to determine the degree of volume strain with deformation. The growth of microvoids in particulate-filled PVC was modelled due to the breakdown of the matrix–particle interface as a function of time. Cavitation was the principal deformation mechanism observed.

Fenelon and Wilson [42] used a volumetric strain approach to study the toughening mechanisms in impact grades of thermoplastics and attempted to relate their results to the expected response to a cavitation or shear-band mechanism.

In all these studies a number of themes emerge. A variety of experimental techniques have been used based on creep measurements, instrumented tensile testing, modified liquid dilatometry and by high-speed optical methods. The principal modes of deformation of either dilation, cavitation, shear yielding or a combination of all three has been studied through a volume strain approach. These mechanisms have been seen in unreinforced polymers, toughened polymers, and composites based on particulate and discontinuous fibre reinforcement, over a wide range of strain rates and temperatures. Thus the technique has a general applicability in studying deformation in polymeric materials and in determining the viscoelastic response of the engineering constants (modulus and lateral contraction ratio) as a function of strain, temperature, time, strain rate, etc.

4. Experimental procedure

The tensile deformation studies of PMMA and 40% talc-filled polypropylene were performed on parallel-sided specimens. The PMMA specimens were taken from cast sheets of the material, and the 40% talc-filled polypropylene specimens were taken from injection-moulded coat-hanger plaques. The 40% talc-reinforced polypropylene material was examined to explore general deformation mechanisms in particulate composites and for comparison purposes to the unreinforced PMMA. The specimens for each test had lengths of approximately 150 mm, widths approximately 12.5 mm and thicknesses ranging from 3–5 mm. The tests were conducted using a screw-driven Instron 6025 Universal Testing Machine with an environmental chamber. All materials were examined at 23 °C and at higher temperatures with a 1 mm min^{-1} crosshead displacement rate. The load applied during extension was monitored using a load cell, the axial strain by using an Instron extensometer and the width strain was recorded using a clip-on horseshoe extensometer. The signals from the load cell and axial extensometer were passed through the Instron 6025 console, then passed through to a HP2240 A/D converter, together with the signal from the width horseshoe extensometer after this had previously passed through a Phillips Bridge. The combined load, axial and width signals were then digitized by the A/D converter, collecting the signals from all channels in a 40 ms time sweep, and finally passed to a HP9816 computer, where they were stored. The resultant data files were finally transferred to a PC computer and analysed using the Lotus 123V3 spreadsheet program. This allowed for the point by point calculation of the tensile modulus, lateral contraction ratio and volume strain, using Equations 7, 2 and 1, respectively, as a function of the applied deformation. The tensile modulus for each specimen was determined by a fitted tangent method in the low strain limit (between 0% and 0.2% applied strain) and the lateral contraction ratio was determined by a fitted tangent method in the region of linearity (between 0% and 0.5% axial strain). The lateral contraction ratio data all had correlation coefficients, R^2, better than 0.99. The value for the lateral contraction ratio was then substituted into Equation 5, to give the predicted volume strain response as a function of applied strain.

5. Results and discussion

5.1. Tensile modulus and lateral contraction ratio measurements

The tensile modulus and lateral contraction ratios for the PMMA and the 40% wt/wt talc-filled reinforced polypropylene specimens are reported in Table I. Typical plots of the stress–strain, modulus–strain and lateral (width) to axial strain data for PMMA and 40% wt/wt talc-filled reinforced polypropylene, measured at 23 °C and 1 mm min^{-1} crosshead speed are shown in Figs 3a–c and 4a–c, respectively. The data for the pseudoelastic constants in Table I showed a temperature dependence, typical of viscoelastic materials. The tensile modulus for each material also

TABLE I Average tensile modulus (measured at 0.2% strain) and lateral contraction ratio data for PMMA (measured between 0.0% and 0.5% strain) at 23, 40, 60 and 80 °C, together with the data for 40% talc-filled polypropylene at − 20, 23 and 60 °C

Material type	Temp. (°C)	Modulus (GPa) (0.2%)	LCR
PMMA	− 20	4.80 (0.10)	0.36 (0.01)
	23	3.13 (0.06)	0.37 (0.02)
	40	2.54 (0.07)	0.38 (0.01)
	60	2.28 (0.05)	0.38 (0.02)
	80	2.06 (0.15)	0.40 (0.01)
40% wt/wt talc-filled polypropylene	− 20	7.20 (0.05)	0.25 (0.01)
	23	4.03 (0.30)	0.27 (0.01)
	60	3.00 (0.05)	0.30 (0.01)

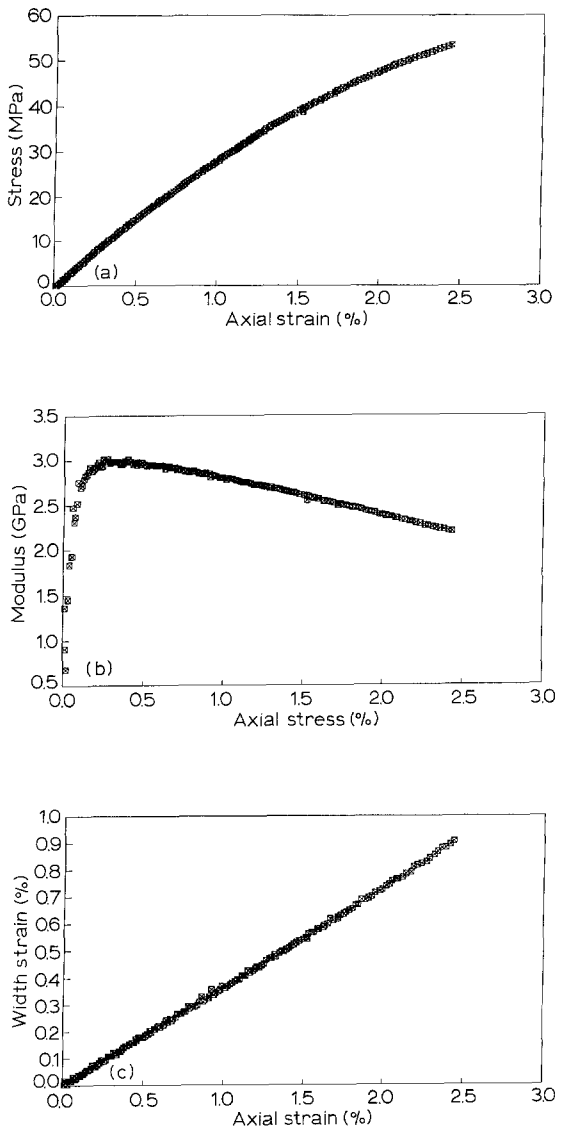

Figure 3(a) Stress–strain data, (b) tensile modulus–strain data, and (c) lateral to axial strain data, for PMMA at 23 °C and at 1 mm min^{-1} crosshead speed, over the range of applied strain.

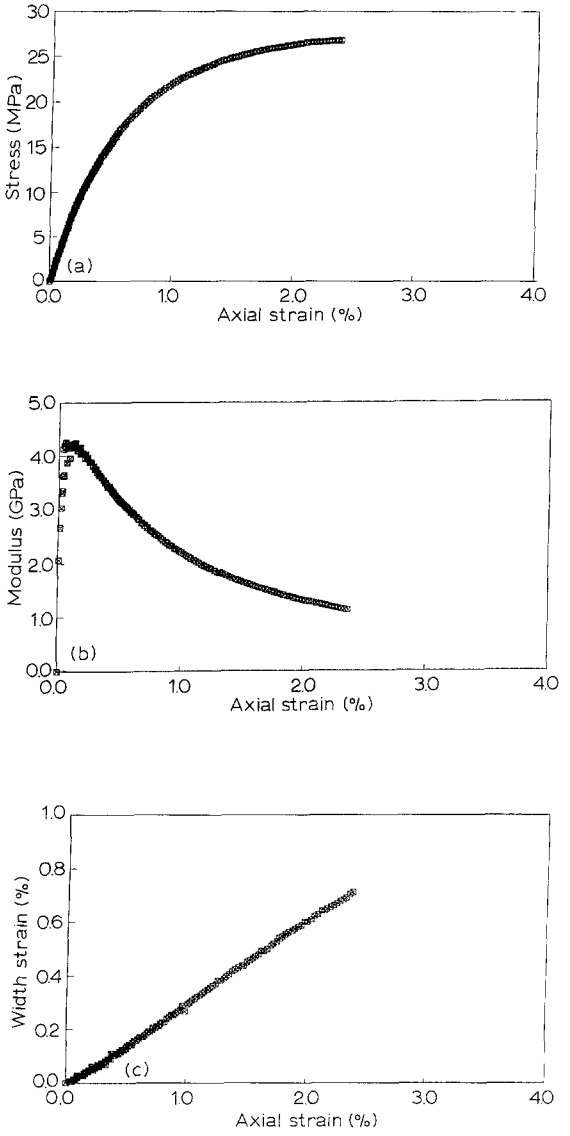

Figure 4(a) Stress–strain data, (b) tensile modulus–strain data, and (c) lateral to axial strain data, for 40% wt/wt talc-filled polypropylene at 23 °C and at 1 mm min^{-1} crosshead speed, over the range of applied strain.

showed a clear dependence upon the level of applied strain. The lateral contraction ratio data also showed a dependence upon temperature and applied strain. These observations are a direct consequence of the viscoelastic nature of polymeric materials [3, 4] and have an important effect upon the deformation. The inherent viscoelasticity also results in a time dependence for these pseudoelastic constants [43]; however, this effect can be ignored for the time under load used in these experiments.

The viscoelastic nature of the pseudoelastic constants for PMMA has been determined by Yee and Takemori [44] in a series of experiments, based on the measurement of dynamic tensile modulus and lateral contraction ratio, using a dynamic servohydraulic technique [45]. The real component of the tensile modulus was found to fall with increasing temperature. A clear increase of the real component of the lateral contraction ratio with temperature, frequency and prestrain was noted. The lateral contraction ratio changed from approximately 0.34 at − 40 °C to 0.365 at 20 °C and finally 0.41 at 100 °C for annealed PMMA; quenched PMMA showed an even larger temperature dependence, rising from 0.36 at − 20 °C to 0.37 at 20 °C and finally 0.44 at 90 °C. Similar results for the temperature dependence of the lateral contraction ratio for PMMA are quoted by Gilmour *et al.* [46], based on a variety of experimental techniques and for other thermoplastics [47, 48]. This result makes interesting comparison to the time dependence of the lateral contraction ratio for PMMA and other thermoplastics, as studied by Benham and McCammond [43] who found that the creep contraction ratio for PMMA rose with increasing time under load and applied stress from 0.40 at 10^2 s to 0.45 at 10^6 s and 38 MPa stress.

The dynamic servohydraulic technique was applied by Yee [49] to the pseudoelastic constants for 40% wt/wt talc-filled polypropylene. The real component of the tensile modulus was found to fall with increasing temperature. The real component of the lateral contraction ratio increased with temperature, from approximately 0.26 at − 20 °C to 0.30 at 20 °C and finally 0.36 at 100 °C.

From the measurements reported in Table I and in the literature, it is clear that the tensile modulus and lateral contraction ratio in polymeric materials are complex pseudoelastic functions, with agreement in the trends that the values have with temperature. The effect of strain and temperature on the volume strain, hence on the deformation mechanisms for the materials studied are discussed next.

5.2. Volume strain measurements

The volume strain data were calculated from the recorded axial and width strain signals recorded in the tensile tests at 23 °C, using Equation 1, assuming that the thickness strain signal was identical to the width strain. The dilational volume strain response for each material was calculated at each value for the axial strain by placing into Equation 5 the low strain value for the lateral contraction ratio. This allowed two functions to be plotted on the volume strain versus axial strain plot. The curve marked by the solid line indicated the dilational response, governed by the lateral contraction ratio; the plotted data points showed the measured volume strain.

Fig. 5 shows the volume strain response for PMMA as a function of applied strain. The comparison between the predicted and experimental data shows that PMMA showed essentially a dilational response, up to 2% strain, beyond which a deviatoric mechanism occurred. At higher temperatures a similar response in PMMA was seen.

Fig. 6 shows the volume strain response for 40% talc-reinforced polypropylene. At low strains there appeared to be good agreement between the predicted and measured response for both materials, indicating that the deformation is governed by the dilational response of the material. At higher strains ($\varepsilon > 0.8\%$), the experimental data showed major departure from the predicted behaviour, finally reaching a constant increase in volume strain with applied strain. This indicates that the material had begun a cavitation-type process at a strain of approximately 0.8%.

The stress data for PMMA plotted against the volume strain is shown in Fig. 7. The response is essentially linear in the low-stress region and the slope of the data can be used to calculate the bulk modulus for the material, as explained in Section 5.3. As noted from Fig. 5, above 2% applied strain PMMA shows a shear-type deformation mechanism. This is equivalent to a stress of approximately 50 MPa, as determined from the stress–strain plot, Fig. 3a. Thus the stress–strain and the volume strain–strain and stress plots can be seen to be interlinked.

The stress–volume strain plot for 40% talc-filled polypropylene is seen in Fig. 8. The response is essentially linear in the low-stress region. Above 20 MPa stress, the volume strain increases rapidly about the yield stress of 27 MPa. The onset of cavitation at 20 MPa stress corresponds to 0.8% strain, identified as the onset of cavitation in the volume strain–axial strain plot of Fig. 6.

The effect of temperature on the volume strain measurements can be seen in the next set of data. The stress–strain plot for PMMA taken at 23 and 80 °C can be seen in Fig. 9, with a typical loss of stiffness recorded at the higher temperature. The volume strain–axial strain plot in Fig. 10 shows essentially the same response at both temperatures across the strain

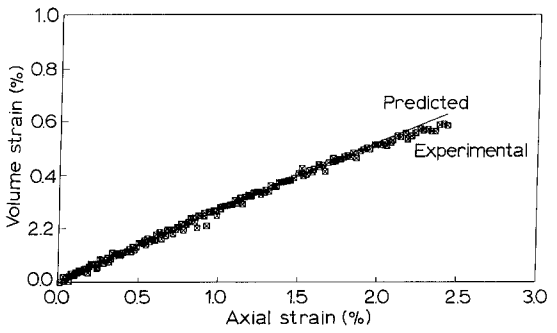

Figure 5 Volume strain versus axial strain plot for PMMA at 23 °C.

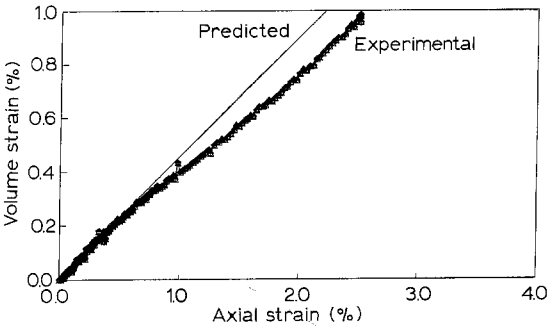

Figure 6 Volume strain versus axial strain plot for 40% wt/wt talc-filled polypropylene at 23 °C.

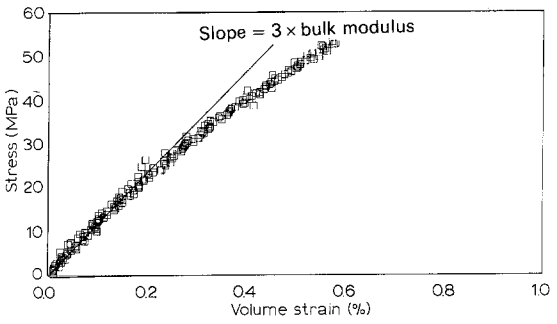

Figure 7 Stress versus volume strain plot for PMMA at 23 °C.

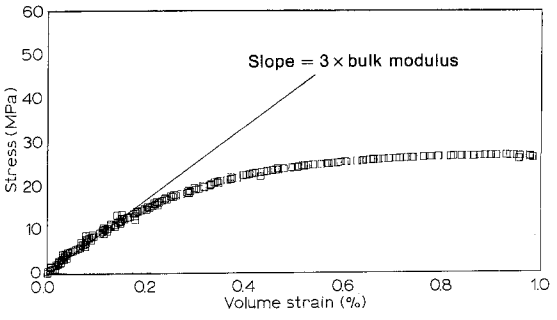

Figure 8 Stress versus volume strain plot for 40% wt/wt talc-filled polypropylene at 23 °C.

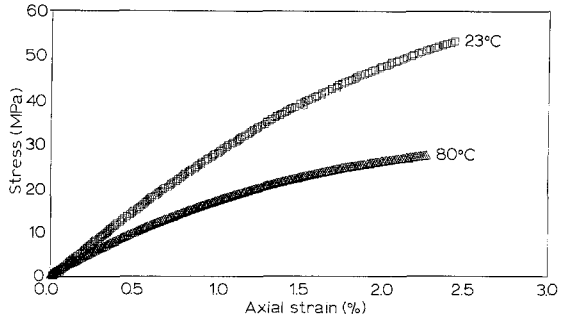

Figure 9 Stress–strain data for PMMA at 23 and 80 °C at 1 mm min^{-1} crosshead speed.

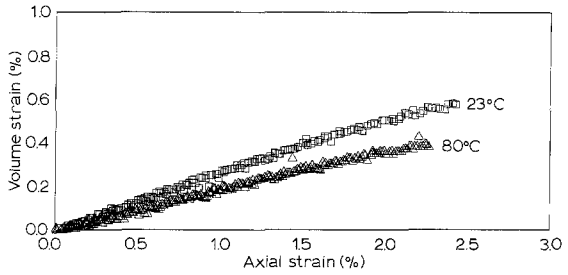

Figure 10 Volume strain versus axial strain plot for PMMA at 23 and 80 °C.

range examined. This is unsurprising because the behaviour is governed principally by the lateral contraction ratio, and although ν slightly increases with higher temperature, the change is not significant enough to produce a large change in the shape of the volume strain with applied strain. In Fig. 11 the volume strain–axial stress plot can be seen. The PMMA test performed at 80 °C showed a yield-type response at about 30 MPa stress; the data for PMMA at 23 °C showed no yield out to 60 MPa as determined from Fig. 9. Similar responses with temperature can be seen in the data for the 40% wt/wt talc-filled polypropylene. In Fig. 12 the stress–strain data at − 20 and 23 °C can be seen. The material has undergone a change between being brittle at the lower temperature to being more ductile at room temperature. The volume strain–axial strain plot in Fig. 13 shows the difference in mechanisms at both temperatures across the strain range examined. The lower temperature data showed only a dilational response, whereas the room-temperature response indicates cavitation occurring. In Fig. 14, the stress–volume strain plot again shows the two mechanisms; dilational (at the lower temperature) and cavitational at room temperature.

5.3. Determination of bulk modulus from volume strain data

As mentioned in Section 1, the bulk modulus for a material is one of the four independent constants that describe the elastic response. The bulk modulus gives a measure of material compressibility when subjected to a state of triaxial compression [1, 2, 5], so that

$$K = -\frac{P}{V_s} \tag{10}$$

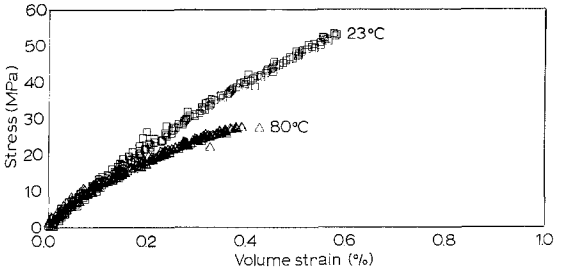

Figure 11 Stress versus volume strain plot for PMMA at 23 and 80 °C.

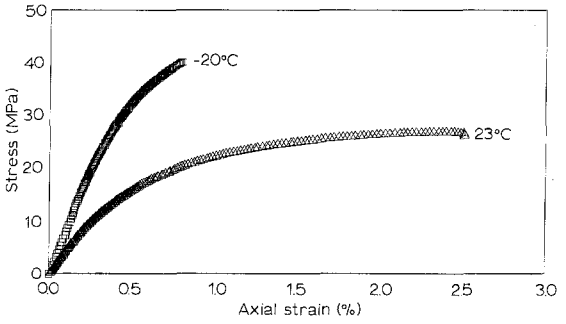

Figure 12 Stress–strain data for 40% wt/wt talc-filled polypropylene at − 20 and 23 °C at 1 mm min^{-1} crosshead speed.

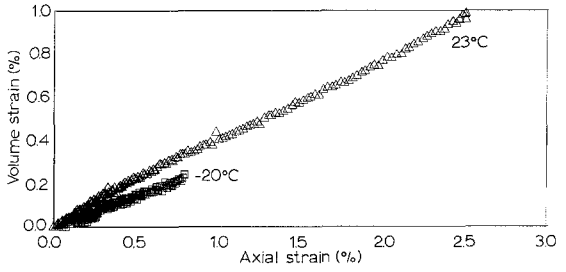

Figure 13 Volume strain versus axial strain plot for 40% wt/wt talc-filled polypropylene at − 20 and 23 °C.

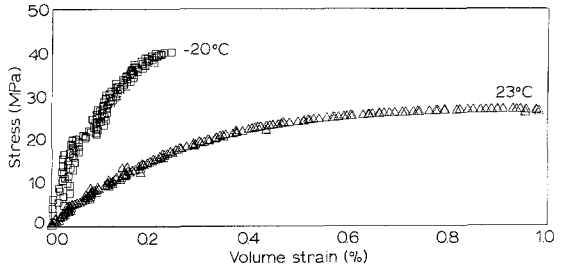

Figure 14 Stress versus volume strain plot for 40% wt/wt talc-filled polypropylene at − 20 and 23 °C.

where P is the triaxial state of pressure and V_s is the resultant volume strain contraction.

More conventionally, the bulk modulus may be expressed in terms of the tensile modulus and lateral contraction ratio

$$K = \frac{E}{3(1 - 2\nu)} \tag{11}$$

If the relationship between volume strain–axial stress is considered and higher order terms in Equation 9 are

ignored, the relationship reduces to

$$V_s \approx \frac{\sigma}{E}(1 - 2\nu) \quad (12)$$

Substitution of Equation 9 into the above volume strain–axial stress relationship gives

$$3K \approx \frac{\sigma}{V_s} \quad (13)$$

so that the measurement of applied axial stress and the resultant strains will result in a direct measure of the bulk modulus in the low deformation limit. Alternatively, the bulk modulus can be calculated using the standard relationship defined by Equation 9.

In Figs 11 and 14, the volume strain–stress response for PMMA and 40% wt/wt talc-filled polypropylene at 23 °C are shown, respectively. Taking a linear fit to the low stress data, and equating this slope m, to the bulk modulus, K, as defined in Equation 11, gives

$$m \approx \frac{\sigma}{V_s} = 3K \quad (14)$$

The values for bulk modulus measured from Figs 11 and 14 are given in Table II, together with their calculated values, using the averaged values of tensile modulus and lateral contraction ratio, contained in Table I.

The measured data, taken from Figs 11 and 14 are in reasonable agreement with the calculated values using Equation 9, taken from the data contained in Table I. It is known that slight errors in the value for lateral contraction ratio can produce large variations in the calculated value for the bulk modulus [50, 51]. A variation of 0.01 in the lateral contraction ratio can produce up to 10% variation in the bulk modulus, assuming a constant value for the tensile modulus. Thus calculation of the bulk modulus via Equation 11 might be seen as a better method for using the experimental data than the standard relationship given by Equation 9, given the cumulative errors involved in calculating the tensile modulus and lateral contraction ratio.

6. Conclusion

The four constants used to describe the state of elastic deformation in materials have been introduced, together with the concept of volume strain. This parameter has been derived from first principles and its relationship to the possible modes of deformation in polymeric materials has been described. The volume strain has been shown to be directly related to the applied stress and strain and also to the tensile modulus, lateral contraction ratio and the bulk modulus. Distinctions between the normal dilational response to a uniaxial tensile deformation and the final failure mechanisms of cavitation or shear banding have been made. Experimental data using an instrumented tensile test technique on PMMA and on a 40% talc-filled polypropylene composite have given basic information on the fundamental elastic constants of modulus and lateral contraction ratio data. The volume strain response for these materials has shown that PMMA showed a deviatoric-type response over the temperature ranges explored. The 40% talc-filled polypropylene composite showed significant cavitation beyond a certain applied deformation. Further experiments on different types of polymeric materials at higher temperatures, higher strain rates, or after some cyclic loading might reveal more information on the bulk deformation mechanisms that are present in such materials, and research is planned in this area.

TABLE II Calculated and measured values for the bulk modulus for PMMA and 40% wt/wt talc-filled polypropylene at 23 °C

Material type	Temp. (°C)	Bulk modulus (GPa)	
		via Eq. 11	From slope m
PMMA	23	4.02	4.27
40% wt/wt talc-filled polypropylene filled polypropylene	23	2.92	2.56

Acknowledgements

The authors acknowledge the work of I.Wood on the development of computing software used in capturing and analysing data, also useful discussions with Dr D.R. Moore.

References

1. A. E. H. LOVE, "A Treatise on the Mathematical Theory of Elasticity", 4th Edn (Dover, New York, 1944).
2. S. SOKOLNIKOFF, "Mathematical Theory of Elasticity" (McGraw-Hill, New York, 1956).
3. J. D. FERRY, "Viscoelastic Properties of Polymers" (Wiley, New York, 1961).
4. B. E. READ and G. D. DEAN, "The Determination of Dynamic Properties of Polymers and Composites" (Hilger, Bristol, 1978).
5. J. R. DRABBLE, in "Elastic Constants under Pressure" edited by H. L. D. Pugh (Elsevier, Amsterdam, 1970) Ch. 4.
6. D. HEIKENS, S. D. SJOERDSMA and W. J. COUMANS, *J. Mater. Sci.* **16** (1981) 429.
7. I. M. WARD, "Mechanical Properties of Solid Polymers" (Wiley, 1983).
8. C. B. BUCKNALL, "Toughened Plastics" (Applied Science, London, 1977).
9. C. B. BUCKNALL and D. CLAYTON, *Nature Phys. Sci.* **231** (1971) 107.
10. *Idem, J. Mater. Sci.* **7** (1972) 202.
11. C. B. BUCKNALL, D. CLAYTON and W. KEAST, *ibid.* **7** (1972) 1443.
12. *Idem. ibid.* **8** (1973) 514.
13. C. B. BUCKNALL and I. C. DRINKWATER, *ibid.* **8** (1973) 1800.
14. C. B. BUCKNALL and W. W. STEVENS, *ibid.* **15** (1980) 2950.
15. C. B. BUCKNALL and C. J. PAGE, *ibid.* **17** (1982) 808.
16. C. B. BUCKNALL, D. CLAYTON and W. KEAST, *ibid.* **19** (1984) 2064.
17. C. B. BUCKNALL, P. DAVIES and I. K. PARTRIDGE, *ibid.* **21** (1986) 307.
18. C. B. BUCKNALL, P. S. HEATHER and A. LAZZERI, *ibid.* **24** (1989) 2255.

19. J. M. HUTCHINSON and C. B. BUCKNALL, *Polym. Engng. Sci.* **20** (1980) 173.
20. M. A. MAXWELL and A. F. YEE, *ibid.* **21** (1981) 205.
21. A. F. YEE and R. A. PEARSON, *J. Mater. Sci.* **21** (1986) 2462.
22. H. J. SUE and A. F. YEE, *ibid.* **24** (1989) 1447.
23. R. A. PEARSON and A. F. YEE, *ibid.* **26** (1991) 3828.
24. W. J. COUMANS and D. HEIKENS, *Polymer* **21** (1981) 957.
25. W. J. COUMANS, D. HEIKENS and S. D. SJOERDSMA, *ibid.* **21** (1981) 103.
26. M. E. J. DEKKERS and D. HEIKENS, *J. Appl. Polym. Sci.* **28** (1983) 3809.
27. *Idem., ibid.* **30** (1985) 2389.
28. *Idem, J. Mater. Sci.* **20** (1985) 3873.
29. M. E. J. DEKKERS, S. Y. HOBBS and V. H. WATKINS, *ibid.* **23** (1988) 1225.
30. S. Y. HOBBS and M. E. J. DEKKERS, *ibid.* **24** (1989) 1316.
31. C. J. HOOLEY, D. R. MOORE, M. WHALE and M. J. WILLIAMS, *Plast. Rubb. Proc. Appl.* **1** (1981) 345.
32. I. T. BARRIE, D. R. MOORE and S. TURNER, *ibid.* **3** (1983) 365.
33. D. C. LEACH and D. R. MOORE, *Composites* **16** (1985) 113.
34. R. S. BAILEY, D. R. MOORE, I. M. ROBINSON and P. M. RUTTER, to be published in "Science and Engineering of Composite Materials".
35. R. W. TRUSS and G. A. CHADWICK, *J. Mater. Sci.* **11** (1976) 111.
36. *Idem, ibid.* **11** (1976) 1385.
37. L. C. CESSNA, *Polym. Engng. Sci.* **14** (1974) 696.
38. J. M. POWERS and R. M. CADDELL, *ibid.* **12** (1972) 432.
39. A. LAZZERI, G. LEVITA and A. MARCHETTI, in "Deformation and Fracture of Composites", UMIST, Manchester, 25–27 March 1991 (Plastics and Rubber Institute, London) paper 28.
40. O. FRANK and J. LEHMANN, *Coll. Polym. Sci.* **264** (1986) 473.
41. R. J. M. BORGGREVE, R. J. GAYMANS and H. M. EICHENWALD, *Polymer* **30** (1989) 78.
42. P. J. FENELON and J. R. WILSON, *ACS Div. Org. Coat. Plast. Prepr.* **34** (1974) 326.
43. P. R. BENHAM and D. McCAMMOND, *Plast. Polym.* (1971) 130.
44. A. F. YEE and M. T. TAKEMORI, *J. Polym. Sci. Polym. Phys. Ed.* **20** (1982) 205.
45. M. T. TAKEMORI, "Dynamic Poisson's Ratio: A Novel Technique to Study Interfacial Adhesion", GE Report 78CRD029, February 1978.
46. I. W. GILMOUR, A. TRAINOR and R. N. HAWARD, *J. Appl. Polym. Sci.* **23** (1979) 3129.
47. I. KRAUSE, A. J. SEGRETO, H. PRZIREMBEL and R. L. MACH, *Mater. Sci. Engng* **1** (1966) 222.
48. L. E. NIELSEN, *Trans. Soc. Rheol.* **9** (1965) 243.
49. A. F. YEE, *Polym. Engng. Sci.* **25** (1985) 923.
50. W. KOSTER and H. FRANZ, *Metall. Rev* **6** (1961) 1.
51. R. J. CROWSON and R. G. C. ARRIDGE, *Polymer* **20** (1979) 747.

Received 24 January
and accepted 6 July 1992